Rapisarda, M., Hernández, J. A., Gatto, A., Parolari, P., Boffi, P., Svaluto Moreolo, M., Fábrega, J. M., Nadal, L., Martínez, R., López, V., Fernández-Palacios, J. P., Otero, G. & Larrabeiti, D. (2022). All-optical aggregation and distribution of traffic in large metropolitan area networks using multi-Tb/s S-BVTs. *Journal of Optical Communications and Networking*, 14(5), 316-326.

DOI: 10.1364/jocn.448115

All-optical Aggregation and Distribution of Traffic in Large Metropolitan Area Networks using multi-Tb/s S-BVTs

MARIANGELA RAPISARDA[1], JOSÉ ALBERTO HERNÁNDEZ[2,*], ALBERTO GATTO[1], PAOLA PAROLARI[1], PIERPAOLO BOFFI[1], MICHELA SVALUTO MOREOLO[3], JOSEP MARIA FÁBREGA[3], LAIA NADAL[3], RICARDO MARTÍNEZ[3], VÍCTOR LÓPEZ[4], JUAN-PEDRO FERNÁNDEZ-PALACIOS[4], GABRIEL OTERO[2], AND DAVID LARRABEITI[2]

[1] *Dipartimento di Elettronica, Informazione e Bioingegneria, Politecnico di Milano, Italy*
[2] *Department of Telematics Engineering, Universidad Carlos III de Madrid, Spain*
[3] *Centre Tecnologic de Telecomunicacions de Catalunya (CTTC/CERCA), Spain*
[4] *Telefonica I+D, Spain*
[*] *Corresponding author: jahgutie@it.uc3m.es*

Current MAN architectures are based on a number of hierarchical levels that aggregate traffic toward the core at the IP layer. In this setting, routers are interconnected by means of fixed transceivers operating on a point-to-point basis where the rates of transceivers need to match. This implies a great deal of intermediate transceivers both to collect the traffic, groom and send it to the core. This article proposes an alternative scheme based on sliceable bandwidth variable transceivers (S-BVTs) where the slice-ability property is exploited to perform the aggregation of traffic from multiple edges n-to-1 rather than 1-to-1. This approach can feature relevant cost reductions through IP off-loading at intermediate transit nodes but requires viable optical signal-to-noise ratio (OSNR) margins for all-optical transmission through the network. In this work we prove through simulation the viability and applicability of this technique in large metro networks with a VCSEL-based S-BVT design to target net capacities per channel of 25 Gb/s, 40 Gb/s, and 50 Gb/s. The study reveals that this technology can support most of the paths required for IP offloading after simulation in a semi-synthetic topology modelling a 20-million inhabitant metropolitan area. Moreover, OSNR margins enable the use of protection paths (secondary disjoint paths) between the target node and the core, much longer than primary paths both in terms of number of intermediate hops and kilometers.

1. INTRODUCTION

Metropolitan area networks (MANs) are in charge of collecting business, residential and mobile traffic of end users at the central offices spread across cities and towns. Typically, MANs are arranged in a hierarchical aggregation/distribution structure where most traffic goes from edge nodes to metro-core nodes, which provide wide area networks (WANs) transit (including Internet access) and content distribution network (CDN) services and caching. In the metro segment, annual traffic growth rates between 25% and 40% are expected for the next years, as a consequence of the emergence of new services related with the arrival of 5G, Internet of Things (IoT), Connected Industry 4.0, and the Cloud paradigm, among others [1–3].

In this context, telcos are required to cope with such traffic growth while featuring ultra-low latency and capital and operational expenditures (CAPEX/OPEX) reductions. In addition, MAN nodes are expected to be equipped with data center capabilities (computing and storage resources) to provide better quality of experience to both users and IoT *things*, estimated as 75 billion connected devices [4–6].

To cope with both performance and cost-effectiveness requirements, both vendors and research community are looking

for scalable low-cost solutions in all scenarios, in particular, in the metro segment. The largest cost percentage resides in the transceivers and transponders interfacing the IP/MPLS routers in the MAN topology. Even small cost-savings in transponders may translate into large global cost savings, especially for telcos operating multiple MANs worldwide [7, 8]. Several optical transport technologies have recently appeared focusing on these challenging techno-economic objectives; two of them are of special interest, namely point-to-multipoint optical transport solutions (widely known as XR-optics) [9–11] and VCSEL-based Sliceable Bandwidth Variable Transponders (S-BVTs) [12, 13].

In this sense, EU H2020 project PASSION[1] focuses on the design of sliceable bandwidth/bitrate variable transceivers (S-BVTs) with integrated vertical-cavity surface-emitting lasers (VCSELs) and coherent reception. S-BVT technologies have demonstrated the ability to generate multiple optical flows that can be routed into different media channels, allowing to flexibly set the optical paths between two endpoints through the optical networks [14]. However, most proposals are based, in the subcarrier generation, on either array of independent laser sources or a single multiwavelength source externally modulated by high-speed IQ modulators [15, 16]. In our proposal we instead exploit direct modulation (DM) of InP VCSELs providing a high-modulation bandwidth, targeting above 18 GHz, and operation within the C-band in a cost-effective manner [17], [18]. Moreover we exploit coherent reception to ensure higher robustness against chromatic dispersion (CD) with respect to direct detection, allowing longer achievable reach. Due to DM, the transmitted signal is just intensity modulated and then a simplified coherent receiver can be used avoiding phase and frequency recovery, reducing the complexity of the receiver DSP and also relaxing the constraints on VCSEL and local oscillator (LO) linewidths [19]. This enables to support up to 50 Gb/s per S-BVT flow generated with DM-VCSELs, thanks to the adoption of multicarrier modulation, and enhanced reach to provide support for long-distance MAN lightpaths [12]. Particularly, a modular and scalable system architecture based on DM-VCSELs at long wavelength and photonic integrated circuits (PICs) has been presented as a novel, low-cost and power-efficient solution to operate in the metro scenario [12, 13, 20]. Although on the receiver side the solution requires a LO source, at the transmitter side external modulators and high-power drivers can be spared. The proposed modular system could then represent a trade-off between cost and flexibility, achieving a reconfigurable flexible-rate transponder that is a contending alternative for incrementally deploying the networks, with respect to other SBV-T technologies [21]. The proposed architecture, programmable via software defined networking (SDN), has been assessed in a real network testbed across multiple nodes, showing a promising performance over multi-hop connections up to 160 km [12]. The SDN-enabled VCSEL-based photonic system has also been demonstrated for spectral/spatial connectivity in disaggregated optical metro networks [22].

On the other hand, the slice-ability feature allows to perform multiple connections of variable capacity with a single transceiver. For example a single S-BVT can simultaneously provide connectivity to a neighbouring router, to the immediately higher node in the hierarchy and/or from the lower level aggregation node toward a metro-core node, offloading the transit level nodes. Thanks to its modular approach, capacity upgrades can be attained by exploiting the spectral resource over the C-band to feature up to 8 Tb/s. Additionally, further upgrade to ultra-high capacity (above 100 Tb/s) can be achieved considering the spatial dimension. The new technological approach and the pay-as-you-grow model are particularly suitable for the adoption of the proposed programmable VCSEL-based S-BVTs in future disaggregated optical metro networks.

After providing experimental preliminary proof of concepts of the proposed VCSEL-based S-BVTs [12, 22], this article shows its applicability to enable long-reach all optical connections between access nodes (central offices) and metro/core nodes in a very large yet realistic MAN scenario serving more than 20 million subscribers. This way, intermediate aggregation nodes may be all-optically by-passed, thus reducing CAPEX investments at the IP layer, namely high-end routers and intermediate transceivers. In this view it is important to study the actual provisioning of the network light paths by evaluating the impairments accumulated by the signals travelling a variety of distances and number of nodes and to analyse the capacity of adaptation of the proposed architecture [23]. We then show that the proposed technology offers good optical signal-to-noise ratio (OSNR) margins at 50 Gb/s, 40 Gb/s, and 25 Gb/s per wavelength (up to 160 wavelengths) and it can support MAN networks with diameters of several hundred of kilometers.

The remainder of this work is organised as follows: Section 2 discusses the global objective of IP offloading of intermediate aggregation metro nodes in a realistic MAN topology of reference. Section 3 overviews the proposed system, adopting the VCSEL-based S-BVTs under development within the EU PASSION project. Section 4 further characterises their main physical/hardware features and provides a detailed characterisation from an OSNR point of view. Section 5 evaluates the suitability of this technology to provide full IP offloading in a very large MAN scenario. Finally, Section 6 summarises this work with its main findings and conclusions.

2. IP OFFLOADING IN LARGE MAN SCENARIOS

Nowadays, MAN design heavily relies on multi-layer technology featuring IP routers on top of reconfigurable optical add/drop multiplexers (ROADMs). Essentially, a router of hierarchical level (HL) n is logically connected (using an optical channel) to one or two routers at the next hierarchical level $n+1$. Such one-hop IP/logical connectivity translates into traversing multiple ROADMs in the optical layer. Ring and/or horseshoe physical topologies commonly appear in lower hierarchical levels, while higher levels are often structured in meshed architectures.

The MAN hierarchy [24] used in PASSION's architecture is shown in Fig.1.

Nodes in this reference MAN belong to one of five hierarchical levels (HLs). The top layer is made up of two HL1 nodes that provide redundant WAN connectivity and a few HL2 nodes (four in the case of our reference topology) that host CDN services (IPTV, content caching, telephony, etc.) and whose purpose is reducing the WAN traffic and the application service latency. Since both HL1 and HL2 are the top gateways of most MAN traffic and the only practical difference between HL1 and HL2 nodes is the availability of WAN links, we shall use HL1/HL2 (or HL1/2) to refer to the MAN core level. HL3 is the transit level that aggregates the traffic from HL4 nodes. HL4 are large central offices (COs) that aggregate traffic from HL5 access nodes (such

[1] "Photonic technologies for progrAmmable transmission and switching modular systems based on Scalable Spectrum/space aggregation for future agIle high capacity metrO Networks", see https://www.passion-project.eu/, last access MAy 2021

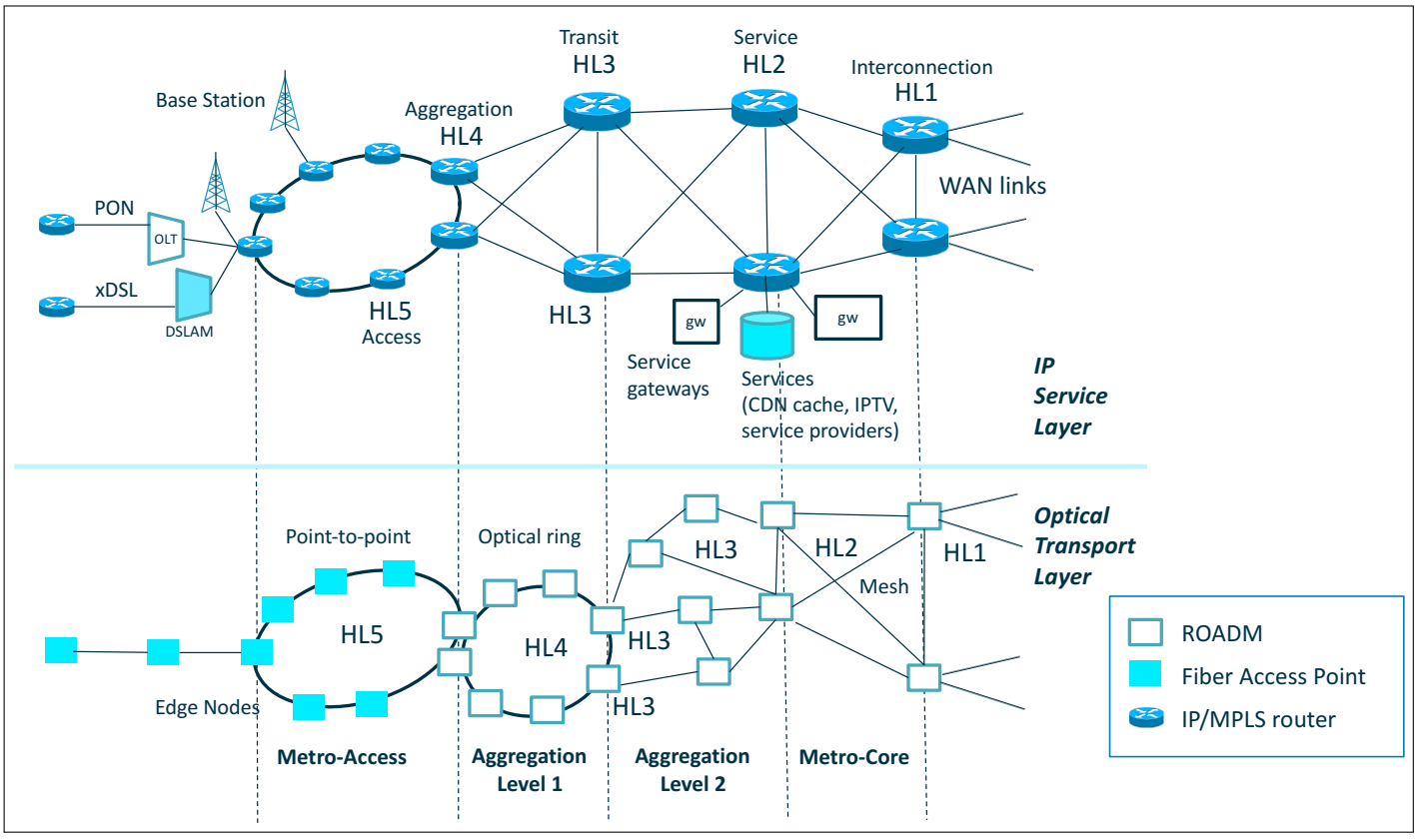

Fig. 1. Hierarchical structure of a 5-level MAN topology

as mobile base stations and other small points of presence).

At the physical layer, from top to bottom, the topology of the core is a mesh and the successive layers underneath are made up of recursive or interconnected rings or horseshoes [25]. At the service or IP logical layer, routers are interconnected by a mesh at HL1/2 level, and by a dual tree structure at HL3, HL4, and HL5 levels as sketched in the scheme. In other words, each HL4 node is logically connected to two HL3 nodes, and each HL3 node is connected to two HL1/HL2 nodes using disjoint links. For simplicity, the real amount of nodes of each hierarchical level is not represented in the picture.

All this logical connectivity can be achieved with a single S-BVT per router. Slice-ability allows to perform multiple connections of variable capacity with a single transceiver. In particular, at HL4 level 2-Tb/s SBVTs with down to 50 GHz spacing are envisioned, whereas at HL3 level 8-Tb/s SBVTs are employed and a 25-GHz spacing is obtained thanks to single side-band (SSB) modulation [12]. In Fig. 2(a), a single S-BVT at an HL4 router can provide connectivity to either a neighbouring router, to the immediately higher node in the hierarchy (HL3) or create shortcuts to the core, at the same time. However, the most interesting multi-connection setting is when high capacity S-BVTs at HL1/2 nodes hub connections to many HL4 nodes whenever possible (Fig. 2(b)). This is because a large percentage of traffic is hierarchical (estimated about 90%). Traffic is aggregated toward the top level (HL1/2) from HL5 into HL4 and HL3 nodes. Once in the core level, the traffic is disaggregated into CDN traffic that remains in the core and WAN traffic (through HL1 routers) that includes: Internet, CDN cache interconnection, VPN and mobile/fixed telephony traffic. Given the current amount of traffic demand in the edge HL5 nodes (20 Gb/s is the currently

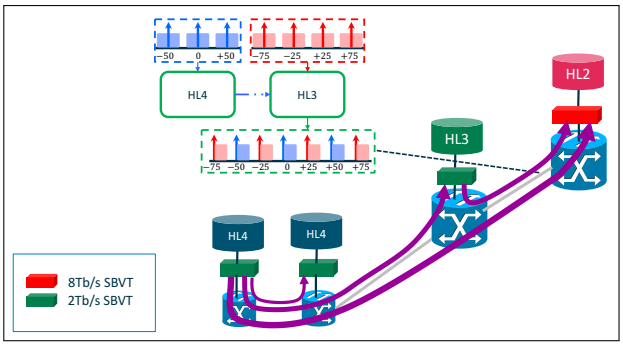

(a) multi-connection stemming from an HL4 node

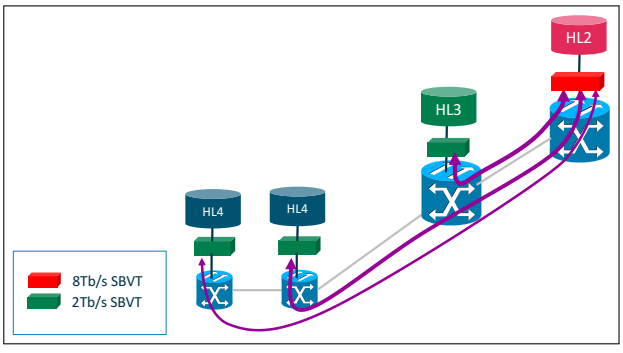

(b) multi-connection stemming from a metro core node (HL1 or HL2) for hierarchical traffic

Fig. 2. Sample S-BVT slicing options in the MAN

recommended backhaul capacity for 5G), aggregation and multiplexing at the optical layer is not cost-effective. Hence the switching and grooming of traffic from HL5 nodes should be electronic (based on IP/Ethernet). WDM multiplexing is more likely to start in HL4. Therefore, HL4 seems to be the appropriate place for the S-BVTs to be deployed.

The rationale to use S-BVTs in the MAN comes from the aggregation/distribution nature of most MAN traffic, since sliceable transceivers natively feature hub-and-spoke connectivity. Fig. 2 shows the flexibility provided by the multi-connectivity capability of S-BVTs. Most HL4's S-BVT optical channels can be destined to the corresponding HL1/2 core node and, as an option, a few channels can be used for shorter connectivity applications. This will usually be neighbour-to-neighbour or HL4 to HL3 circuits (see Fig. 2.(a)). These smaller circuits can serve to carry especial traffic with ultra-low-latency requirements, such as 5G fronthaul interface traffic [26], or to provide inter-edge-data center protection [27, 28].

However, the configuration that makes the most of S-BVT devices in an aggregation/distribution scenario such as a MAN is the one depicted in Fig. 2.(b), where a high capacity S-BVT at HL1/2 hosts connections, using bundles of optical channels, to lower capacity S-BVTs at HL3 and HL4 nodes. Furthermore, if the transmission and switching technology supports all optical HL4-HL1/2 circuits it is possible to save many resources through IP offloading. This is illustrated in Fig. 3. On the one hand, Fig. 3.(a) shows a Fixed Transponder (FT) based conventional IP/WDM logical interconnection of routers. This requires high-end routers at HL3 and multiple FTs to aggregate the traffic of HL4s as well as to forward the traffic to HL1/2. On the other hand, Fig. 3.(b) shows the concept of IP offloading at HL3 enabled by S-BVTs. Here, the optical circuits skip the intermediate HL3 IP hop. In the PASSION design, each HL1/2 node would be equipped with 8 Tb/s or 16 Tb/s S-BVTs with a granularity of 50 Gb/s (each individual optical channel). These carriers are dynamically allocated and bundled by the SDN control plane according to the current demand of HL4 nodes. Three main advantages of this approach are: a) the saving of IP routers at HL3, which may be removed or replaced by less expensive HL4 routers, b) the saving in router interfaces and FTs and finally, c) lower latency and jitter through the MAN thanks to statistical multiplexing at the optical layer.

At the physical layer, however, this logical connection requires the traversal of a number of intermediate ROADMs before reaching the HL1/2 routers, which is very challenging [24].

In this context, the target is to achieve valid all-optical bidirectional channels from edge MAN nodes (HL4) to core MAN nodes (HL1/2) including both link-and-node-disjoint primary and backup paths. The viability of those multi-level direct paths is given by their OSNR.

Fig. 4(a) shows the primary and secondary paths protecting the connectivity of HL4 routers to the core with two horseshoe stages. Each optical path from each HL4 terminates at an end of the horseshoe (an HL3 node). Then the HL3 router aggregates all the traffic from the 6 HL4 depending on it and forwards the traffic over a bigger 1.2Tb/s optical channel from the HL3 to the core. The selection of this capacity assumes an over-subscription 2:1. The picture also shows the need for 6x400Gb/s FTs at the HL3 node to support the HL4 in the horseshoe. This short-range vision of protection vastly employed in the state of the art can be enriched with the possibility of protecting connectivity across several hierarchical levels, rather than protecting the connectivity just to the adjacent layer. Fig. 4(b) illustrates the concept of

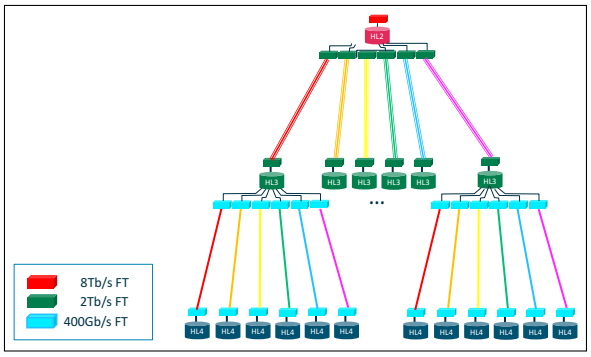

(a) IP-over-WDM using Fixed Transceiveres

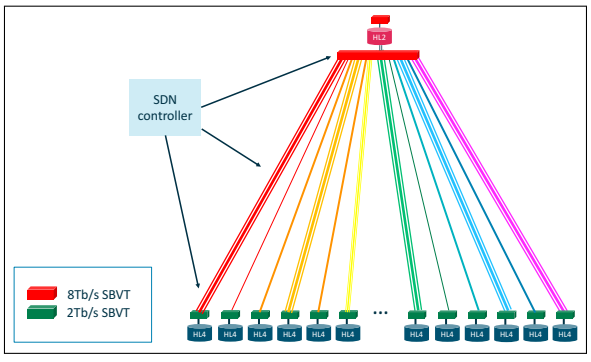

(b) Architecture with S-BVTs and SDN

Fig. 3. (a) Proliferation of transceivers in the MAN with IP over WDM using fixed transceivers ; (b) Statistical multiplexing at the optical layer enabled by sliceable bandwidth-variable transceivers and SDN

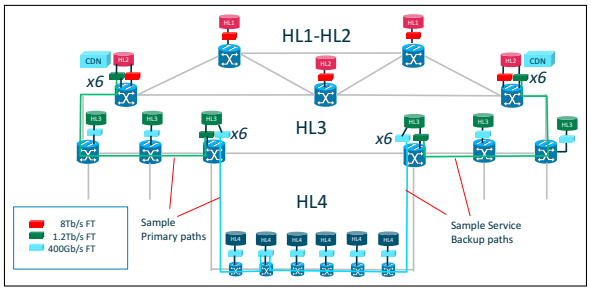

(a) IP-over-WDM wiht Fixed Transceivers

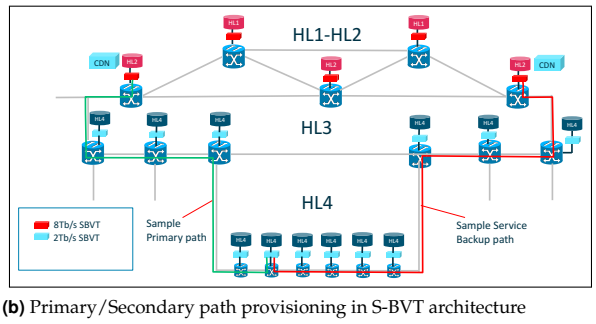

(b) Primary/Secondary path provisioning in S-BVT architecture

Fig. 4. Service protection: (a) IP over WDM with fixed transceivers: ring or horseshoe protection; (b) Concept of primary and secondary paths between hierarchical levels in IP off-loading scenario with sliceable bandwidth-variable transceivers

primary and secondary paths used in this paper. As it can be seen, each HL4 is connected to the closest HL1/2 router over a primary path (in the picture, to the west) which is protected by another HL4-HL2 secondary path (in the picture, to the east). The primary HL4-HL1/2 path is the shortest path connecting the HL4 and any HL1/2 node in the core, whereas the secondary or protection path of the primary one is the shortest path physically disjoint to the primary. Consequently, the target is not reaching an alternative HL3 node, but a high capacity S-BVT hub node at any HL1/2 node. Rather than static over-subscription and IP multiplexing, the availability of a smart control plane adjusts the capacity of primary and backup paths to the current demand of each HL4 node with a 50Gb/s granularity. The HL4 2Tb/s S-BVTs represented in Fig. 4(b) fit the use of the optical capacity to the IP traffic demand (mininum 50Gb/s) whereas Fig. 4(a) HL4 FTs occupy 400Gb/s in HL4-HL3 irrespective of the traffic.

Again, the comparison of Fig. 4 (a) protection with IP/WDM vs (b) S-BVT protection reveals the saving in transceivers and router switching power due to the use of an intermediate hop HL3, which shows the importance of IP by-passing in the hierarchy and all optical end-to-end HL4-HL1/2 paths. This will be further shown in Section 5.

3. VCSEL-BASED S-BVT SYSTEM

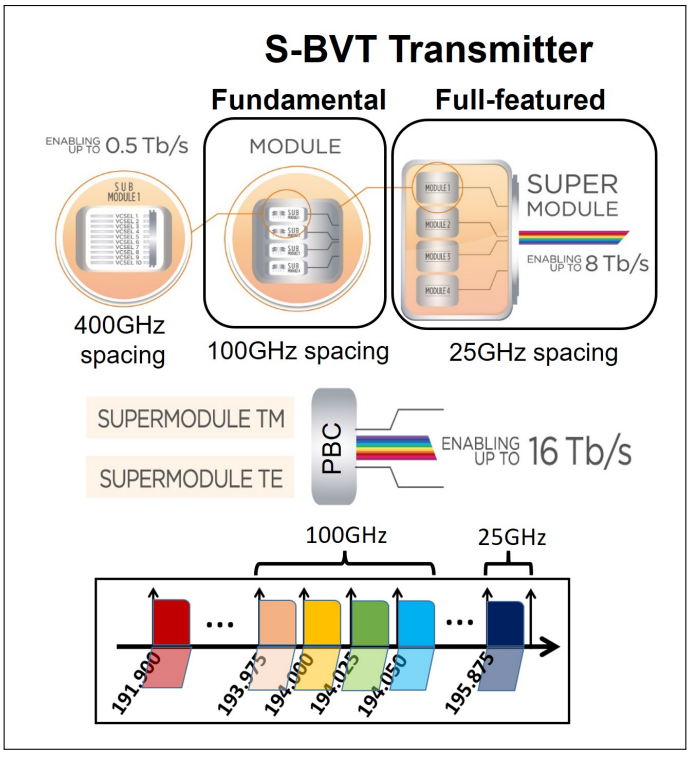

Fig. 5. S-BVT transmitter module composition and corresponding VCSEL operating wavelengths/channels.

This section provides an overview of the proposed system architecture adopting VCSEL-based S-BVTs. The transceiver is based on integrated VCSELs and coherent reception, according to the technologies developed within the context of EU H2020 PASSION project. As stated in the introduction, the VCSEL technology cost-effectively allows high modulation bandwidth and C-band operation, while coherent reception is adopted in order to achieve larger reach thanks to its higher robustness against CD with respect to direct detection [13]. Thus, this enables to cover the targeted large MAN paths at 50 Gb/s per flow [12]. Each flow is generated by directly modulating the VCSELs adopting multicarrier modulation, either discrete multitone (DMT) or orthogonal frequency division multiplexing (OFDM). Multiple flows (up to 40) can be activated/aggregated within a single integrated S-BVT module, which is composed of 40 VCSEL sources, very stable in polarization [29]. This module is constituted of 4 submodules integrated on a silicon-on-insulator (SOI) chip. Each submodule integrates 10 InP short-cavity VCSELs at operating wavelengths within the C-band. The channels generated by the VCSELs of each submodule are spaced between each other of 400 GHz, while the operating wavelengths of the different submodules are spaced apart among each other of 100 GHz. As an example, the first VCSEL of the first submodule operates at 191.900 THz and the second VCSEL of the first submodule operates at 192.300 THz, while the first VCSEL of the second submodule operates at 192.000 THz. Thus, the 40 VCSEL sources are multiplexed (and suitably interleaved) within the PIC module adopting arrayed waveguide grating (AWG) technology, so that the operating wavelengths result in 100-GHz spacing. The 40-VCSEL PIC operates at constant temperature thanks to a single thermoelectric cooler for an active cooling control in order to prevent the wavelength shift of the VCSELs emission [30]. The 40-VCSELs integrated module is the fundamental S-BVT element enabling up to 2 Tb/s per polarization (50 Gb/s per VCSEL flow) and it is used to equip low hierarchical level (HL4) nodes. Thanks to the modular approach, an easy upgrade to higher capacity can be enabled by suitably adding modules. Specifically, exploiting the C-band in the range 191.900 THz - 195.875 THz (corresponding to the ITU-T grid channels CH19-CH58) may yield up to 8 Tb/s. This is obtained composing the S-BVT with 4 different fundamental modules with interleaved operating wavelengths (super-module), enabling 25GHz-spaced channels (VCSEL flows), as shown in Fig. 5. Considering polarisation division multiplexing (PDM), the outputs of two 8-Tb/s supermodules, orthogonal in polarization, can be combined thanks to a polarization beam combiner (PBC), doubling the capacity (up to 16 Tb/s). By exploiting the spatial dimension with spatial division multiplexing (SDM), above 100 Tb/s can be targeted following this grow-as-needed approach [12]. The metro-core nodes at high hierarchical levels (HL2 and HL1) are equipped with full-featured high capacity S-BVTs. Photonic integration and modularity are key to achieve a cost-effective and scalable system enabling Tb/s capacity over large MANs. This approach is also considered for the design of the switching elements and the node architecture, to keep reasonable the cost of the solution and ease its scalability. In particular, low-priced switches are adopted at the HL4 nodes for simple add/drop functionality. They use 50-GHz AWGs and semiconductor optical amplifiers (SOAs) acting as wavelength blockers (see Fig. 6). At the upper hierarchical levels (HL3 and HL1/2), the nodes are more complex and include additional modules and elements enabling advanced functionalities for handling both the spectral and spatial dimensions [12]. Specifically, 100-GHz multiplexers and wavelength selective switches (WSSs) with 25-GHz granularity are adopted for the spectral switching at the upper hierarchical levels, as illustrated in Fig. 6.

In order to exploit all these resources, a centralised SDN-based controller handles the dynamic routing and spectral resource allocation of connections made up of bundles of m optical channels of 25, 40 and even 50 Gb/s [31] up to a multi-Tb/s of aggregate capacity. The number of dynamically enabled/activated

optical channels setup by the SDN control plane depends on the current traffic demand between the S-BVT and their multiple peers, as illustrated in Fig. 2. However the most challenging and cost-saving connectivity target for S-BVTs is direct all-optical HL1/2-HL4 interconnection (Fig. 3.(b)), which is the focus of this work and whose feasibility is analysed in the next section.

4. OSNR CHARACTERISATION

This section characterises the optical technologies developed within the EU H2020 PASSION project, considering both VCSEL-based transceivers and intermediate nodes, in an attempt to assess whether or not such technologies are suitable to enable direct end-to-end optical lightpaths, both primary and backup ones. The viability of those multi-level direct paths is given by their OSNR.

As shown next, the method to compute the end-to-end OSNR is given in two steps, including the effect of node traversal, fibre propagation and optical amplification. Additional evidence of the validity of this approach through real experiments is summarised in section C.

A. Path OSNR simulations

The viability of primary and backup paths in a large MAN topology is assessed via simulations estimating the impairments caused by the nodes traversal by computing the necessary OSNR to achieve a specified Bit Error Rate (BER). The employed simulation tool has been previously validated with experimental results in case of single side-band (SSB) DM-VCSELs in networks characterised by tight optical filtering [12, 32]. The tool is schematically represented in Fig. 6. In particular, the DM VCSEL is modelled considering its typical linewidth, both the intrinsic modulation properties and the extrinsic device parasitic components and including the chirp parameters measured on the actual devices, following the approach fully detailed in [33]. This allows to precisely estimate the impact of node filtering and crosstalk from adjacent channels with respect to the channel under test (CUT), whereas the the chirp interplay with CD can be neglected thanks to CD digital signal processing (DSP) compensation [33]. The tool computes the minimum OSNR threshold needed to traverse a given number of nodes designed with different architectures in order to achieve a net capacity per channel of 50 Gb/s, 40 Gb/s, and 25 Gb/s, respectively.

The optical signal is transmitted along spans of standard single mode fibre (SSMF) with 0.25 dB/km attenuation amplified by erbium-doped fiber amplifiers (EDFAs) with 6-dB noise figure (NF). Each MAN primary and backup path is associated to an OSNR budget computed with the linear model presented in [34]. The comparison between the OSNR thresholds obtained by the simulation tool with the path OSNR budgets guarantees the feasibility of setting up a specific path, supporting one of the three target capacities. The simulation analysis evaluates the performance of seven 25-GHz spaced WDM channels modulated with an SSB DMT signal crossing MAN nodes at HL4, HL3, and HL1/2 levels. The analysis has been carried out for every possible combination of 11 network nodes, considering that at least one HL3 node is necessary to properly select the desired channel. The adopted HL3 node architecture [35] includes aggregation/disaggregation switches and WSSs which are crossed twice per node when channels need to be dropped/added from the considered optical flow. In the following simulations we supposed that this occurrence takes place at every node, thus taking into account a worst case scenario for the filtering impairments.

As shown in Fig. 6, each channel is generated by an 18-GHz VCSEL, with $\alpha = 3.7$ and $\kappa = 1.526 \cdot 10^{13}$ Hz/W chirp parameters and 0-dBm power. The VCSEL is directly modulated with a 16-GHz DMT signal [19] composed of 256 subcarriers, employing a bias current and a modulation amplitude of 9 mA and 10 mA, respectively. As depicted in Fig. 2.(a), the channels in the HL4 rings are 50-GHz spaced, while at the first HL3 node the channels with 25-GHz spacing are added. In total, seven channels are considered to propagate in the considered MAN networks. The optical noise arising from the amplification by EDFAs is added at the end of the propagation, by properly setting a given level of OSNR. The signal is then coherently detected with a 25-GHz coherent receiver exploiting a 10-dBm per polarisation local oscillator with 100-kHz linewidth. The receiver DSP provides for CD compensation, digital synchronisation, cyclic prefix removal, subcarriers phase recovery, demodulation, and error count. With Chow's bit- and power-loading algorithm [36] the transmitted capacity is computed for a target BER of $3.8 \cdot 10^{-3}$ (as for 7% OH hard decision FEC [37]) and then compared to the target capacity. If the OSNR value allows to achieve one of the given target capacities, it is considered as the minimum OSNR threshold for that given topology, otherwise the OSNR is properly updated.

Table 1 summarises the threshold OSNRs to achieve net target capacities of 50 Gb/s, 40 Gb/s, and 25 Gb/s per channel for several ligthpaths (in terms of number of traversed nodes and their type). Fig. 7 depicts some examples of the dependence of the required threshold OSNRs on the number of crossed: (a) HL4 nodes and (b) HL3-HL1/2 nodes. HL4 node crossing has a moderate impact on the performance, due to a wider filter bandwidth, with respect to HL3 one. Indeed, in the case of HL4 crossing, the OSNR thresholds face a slight improvement due to a more effective vestigial sideband filtering, induced by the cascade of off-centered 50-GHz flat-top AWGs [35]. Fig. 6 shows the spectra of the transmitted CUT (on the left) and of the same channel after crossing 10 HL4 nodes (in the center of the figure): the left sideband is filtered out, while the right one is unaffected by the node crossing. On the other hand, due to its narrow filtering (25 GHz), the effect of HL3 node crossing on the required OSNR is much more evident for an increasing hop number: no more than 5 HL3 nodes can be supported with a net capacity of 50 Gb/s. For 2 HL3 nodes a higher OSNR threshold is necessary with respect to the 3 HL3 case due to a more significant crosstalk of the adjacent channels on the CUT. It is quite straightforward to conclude that, for 40 Gb/s and 25 Gb/s capacities, the OSNR constraints are looser and so up to 10 HL3 nodes can be traversed for a 25-Gb/s net capacity target.

5. EVALUATION

This section shows an evaluation summary of the presented technology in a large and real network topology. The experiments have been conducted using the well-known `igraph` library, available in R and Python.

A. MAN topology description

The topology used for evaluation comprises 419 nodes and 531 links, spanning three hierarchical levels, namely HL4 (380 nodes), HL3 (33 nodes), and HL1/2 (6 nodes); this is a real MAN topology managed by Telefonica in one of the countries it operates, the same one used in the experiments of [12]. Fig. 8 shows histograms of link length (in km) and node degree, with average values being 8.65 km and 2.57 links per node respectively. As

Table 1. OSNR minimum threshold (in dB) to get a transmitted capacity of 50 Gb/s (green), 40 Gb/s (yellow), and 25 Gb/s (pink) as a function of the number of crossed HL4 and HL3 nodes. The blue squares indicate a total number of nodes higher than 11. The grey cells mark the impossibility of reaching such a target capacity. The darker cells pinpoint the MAN path cases with more than 11 hops.

		HL3									
		1	**2**	**3**	**4**	**5**	**6**	**7**	**8**	**9**	**10**
HL4	**0**	33.5	39.2	37.8	39.6	47					
		30	33	32	32.7	33.6	35.1	38			
		23.6	25.6	24.2	24.7	26	26.8	28	28.2	28.6	29.1
	1	33.3	39	37.8	39.6	47					
		29.8	32.8	31.8	32.5	33.4	34.9	37.6			
		23.1	25.1	23.8	24.5	25.9	26.6	27.8	28.1	28.5	28.8
	2	33.1	39	37.7	39.6	47					
		29.6	32.6	31.6	32.5	33.2	34.7	37.4			
		22.8	24.7	23.5	24.2	25.7	26.4	27.7	27.9	28.3	
	3	33.1	39	37.5	39.6	47					
		29.4	32.4	31.4	32.3	33	34.5	37.4			
		22.4	24.1	23	24	25.5	26.2	27.5	27.7		
	4	33.1	38.8	37.4	39.4	46.9					
		29.2	32.2	31.3	32.3	33	34.5	37.2			
		22.2	23.9	22.7	23.8	25.3	26.1	27.3			
	5	32.9	38.6	37.4	39.4	46.9					
		29	32	31.1	32.1	32.8	34.2	37			
		21.9	23.6	22.5	23.6	25.2	26	27.1			
	6	32.9	38.6	37.3	39.2	46.8					
		28.8	31.8	31.1	31.9	32.8		37			
		21.6	23.4	22.3	23.6	25		27.1			
	7	32.9	38.4	37.1	39.2	46.8					
		28.7	31.6	31	31.9	32.8					
		21.4	23.2	22.1	23.5	24.8					
	8	32.8	38.2	37.1	39	46.8					
		28.7	31.6	31	31.9	32.8	34.2				
		21.2	23	21.9	23.4	24.8	26				
	9	32.8	38.2	37	39						
		28.5	31.5	31	31.9		34.2				
		21	22.8	21.8	23.2		26				
	10	32.7									
		28.4									
		20.2									

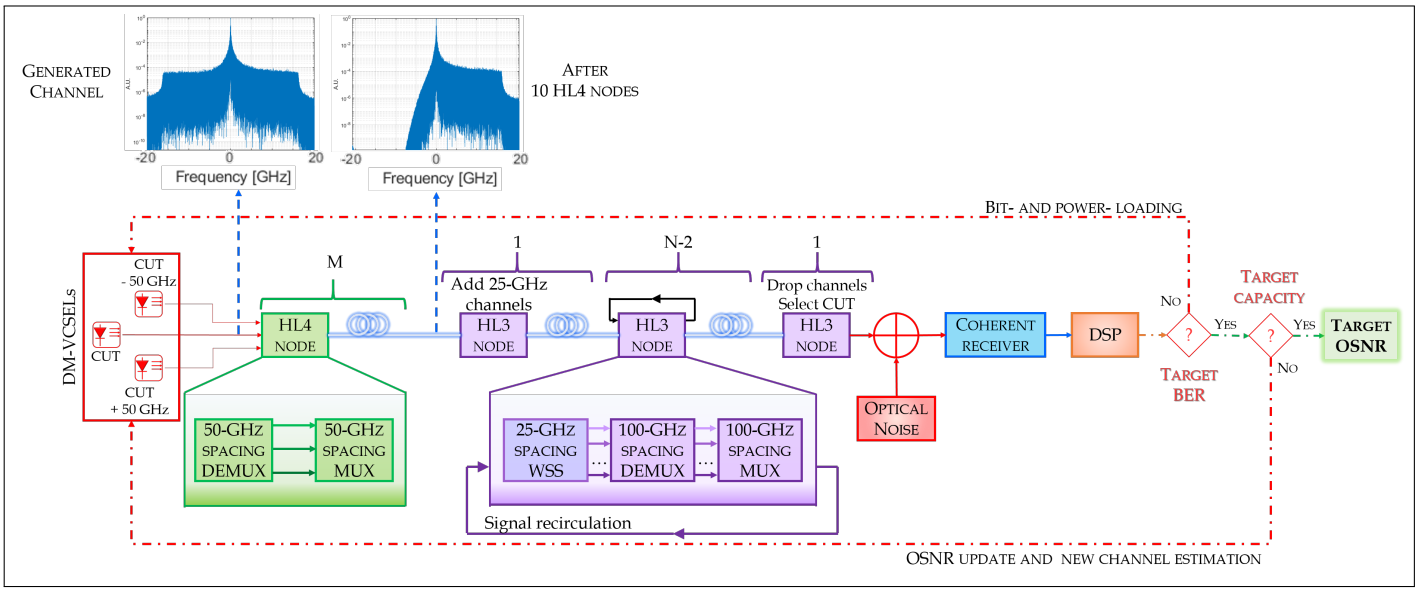

Fig. 6. Schematic of a generic simulation to achieve the target OSNR for M HL4 nodes and N HL3-HL2/1 nodes.

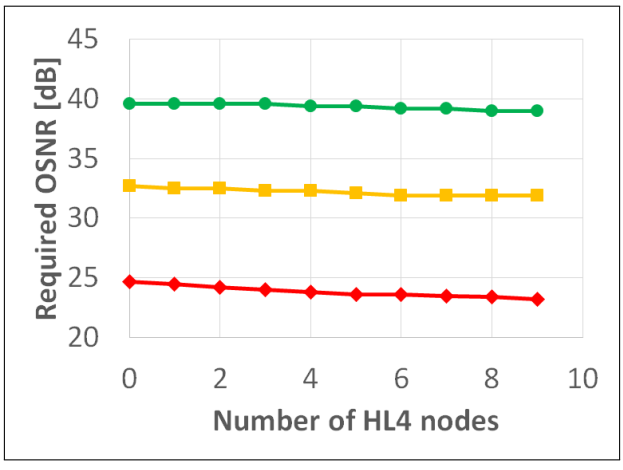

(a) 4 HL3-HL2/1 nodes

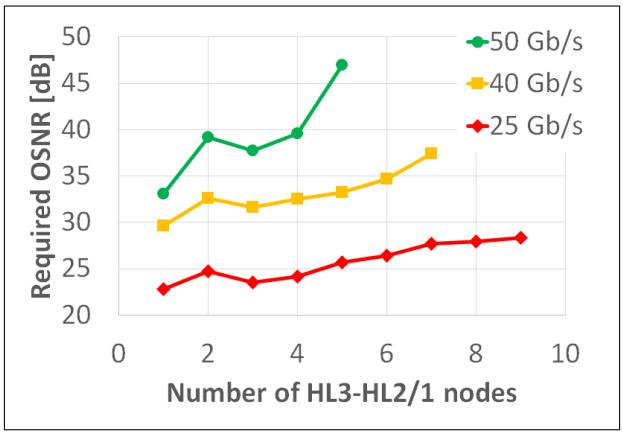

(b) 2 HL4 nodes

Fig. 7. Examples of required OSNRs for given target capacities: (a) 4 HL3-HL2/1 nodes; (b) 2 HL4 nodes.

shown, all link lengths are below the typical 80 km span length, thus optical amplification is directly performed at intermediate nodes.

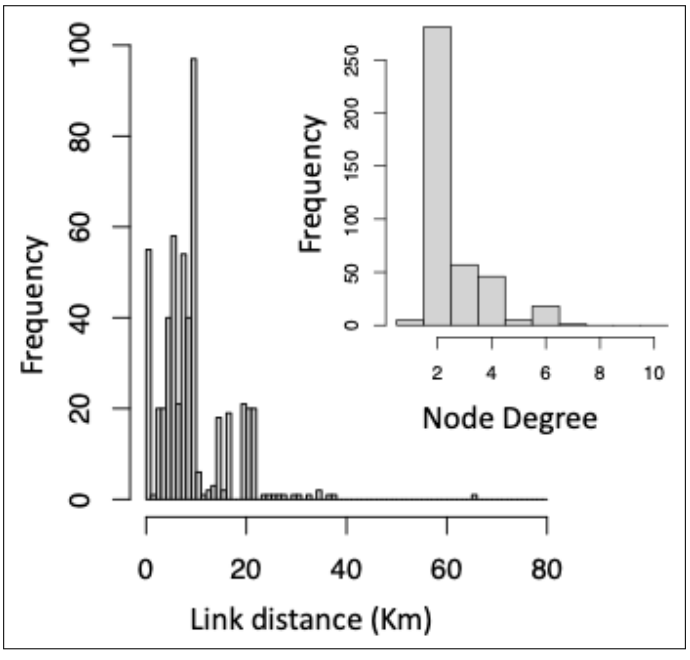

Fig. 8. Link distance and node degree histograms.

B. Primary and backup path computation

On this topology, we computed both primary and secondary (i.e., backup) paths from every access HL4 node to the closest HL1/2 node of all six, using minimum hop count as the routing metric, instead of physical distance, since this is the most limiting aspect according to Table 1. In the case where multiple HL1/2 nodes are at the same distance (i.e., number of hops), we choose the closest HL1/2 node in terms of physical distance in km. This generates 380 HL4-HL1/2 primary paths.

Concerning secondary/backup paths, these are chosen as follows: at first, we remove all nodes (and their associated links) that belong to the primary path except the source. This forces to obtain a backup path which is totally link and node disjoint with respect to the primary path. This strategy also finds the path to the closest HL1/2 destination node, different from the primary path. However if the node removal makes the graph disconnected (second case), preventing to obtain a secondary path, in the computation we allow nodes and links that appear in the primary path but we discourage their use by assigning high metric/cost (i.e., 1000) to these links. Following this methodology, we obtain:

- 238 backup paths are totally disjoint in terms of nodes and links (first case);
- 142 backup paths share at least one node and/or link with the primary path (second case); in particular:
  - 124 of them share 1 node and 0 link with the primary path;
  - 1 path share 1 node and 1 link;
  - 10 paths share 2 nodes and 0 link;
  - 7 paths share 2 nodes and 1 link.

C. OSNR evaluation

Fig. 9 shows the box-and-whisker plots for the number of hops and physical distance (in km) of both primary (green) and secondary (yellow) paths using the methodology explained above. Note that primary paths are obviously closer to the HL1/2 both in number of hops and physical distance than the secondary paths. Boxplots include both the 25th-percentile (1st quartile or Q_1), 50th-percentile (i.e., median or second quartile, Q_2), and 75th percentiles (3rd quartile, Q_3). The whisker and dashed lines represent a distance of 1.5 times the interquartile range (IQR, $Q_3 - Q_1$) above and below the 3rd and 1st quartile respectively. All other points in the dataset outside the whiskers are considered and plotted as outliers (circles).

It is important to notice that primary HL4-HL1/2 lightpaths can take up to 8 hops, while backup lightpaths may require even up to 14. Also, primary paths can require up to 150 km distance, while backup paths may have to traverse up to 200 km. These numbers can give us an idea of how large this MAN topology is.

Concerning the link OSNR, this value depends on both number of hops and distance traversed along the HL4-HL1/2 path, as explained in Section A. Fig. 9 shows that primary paths usually present higher values than secondary paths. This seems reasonable, since primary paths are closer to the destination node both in terms of hop count and physical distance.

In this large topology, the entire set of primary paths complies with the OSNR requirements for supporting 25 and 40 Gb/s. Regarding 50 Gb/s, only 352 primary and 304 secondary paths out of 380 (i.e., 92.63% and 80% respectively) are feasible at 50 Gb/s, i.e., their OSNR required values are below the threshold limits displayed in Table 1. In particular, we observe that:

- 50-Gb/s capacities require an OSNR between 32.8 to 47 dB (min and max), on average 37.80 dB.
- 40 Gb/s requires between 28.50 and 37.20 dB OSNR (min and max), on average 31.67 dB.
- 25 Gb/s requires between 21.00 and 27.30 dB OSNR (min and max), on average 23.55 dB.

As shown in Fig. 9 all primary paths have OSNR values above 38 dB (the minimum obtained value is 38.04 dB), while secondary paths are above 36 dB (minimum value of 36.46 dB). This implies that all the primary and secondary paths support both 40 Gb/s and 25 Gb/s capacities in this topology. However, only 92.63% of the primary lightpaths can be established at 50 Gb/s since the OSNR requirements are substantially higher than at 25 and 40G. This reduces the percentage of paths that can achieve 50 Gb/s to 92.63% and 80% for primary and secondary cases respectively, as it can be derived from Table 1.

D. OSNR evaluation on ultra-large MAN topologies

In a final experiment, we stressed the topology by multiplying each link length by a factor α, i.e., we have the same topology but with longer distances. We recomputed both primary and secondary paths and found the percentage of cases where the 50-Gb/s, 40-Gb/s, and 25-Gb/s capacities are supported. The results are shown in Table 2. As shown, still a large majority of paths are supported even at 2x-3x the end-to-end lightpath distance of the original topology. This conclusion also applies to the case where the shortest route cannot be allocated to a lightpath and an alternative sub-optimal primary path needs to be provisioned. In such a case, the table reveals that still 25, 40 and 50G transmission is possible on longer distances than the optimal one.

Finally, concerning cost savings, under the assumption that IP/MPLS routers have an approximate cost of 768, 364 and 48 normalised Cost Units (CU) for HL1/2, HL3 and HL4 nodes (values taken from Table 3 of [6]), the percentage of cost savings due to HL3 optical bypassing is approximately 34% in IP routing:

$$\frac{364 * 33}{768 * 6 + 364 * 33 + 380 * 48} = 0.34$$

6. SUMMARY AND DISCUSSION

This paper has demonstrated by simulation the feasibility of covering distances up to 200 km in multinode all-optical lightpath scenarios with the proposed low-cost multi-Tb/s VCSEL-based S-BVT system. In particular the OSNR thresholds to achieve 25-Gb/s, 40-Gb/s, and 50-Gb/s net channel capacities have been computed for all possible combinations of at most 11 HL4-HL3-HL1/2 nodes and compared to the OSNRs estimated for several network topologies.

The experiments reveal that indeed HL3 bypassing is possible in all cases, since the OSNR values between HL4-HL1/2 comply with the requirements at all the target channel capacities in a large majority of cases. Furthermore, even in the case of larger topologies in terms of covered distances, all-optical lightpaths between HL4 and HL1/2 are possible in a large percentage of primary and secondary paths, at 25 Gb/s, 40 Gb/s, and even 50 Gb/s in many cases.

This result allows network operators perform all-optical IP offloading of intermediate HL3 nodes, reducing their complexity, latency and CAPEX/OPEX, confirming the capabilities of the proposed multi-Tb/s VCSEL-based modular S-BVT. In fact, removing intermediate IP/MPLS routers can result in important cost savings not only in terms of CAPEX, but also OPEX (site rental, power consumption and operations). Furthermore, the flexibility provided by the S-BVTs with 50G granularity allow to provision traffic demands in a more efficient way than using fixed 100G or 400G transceivers.

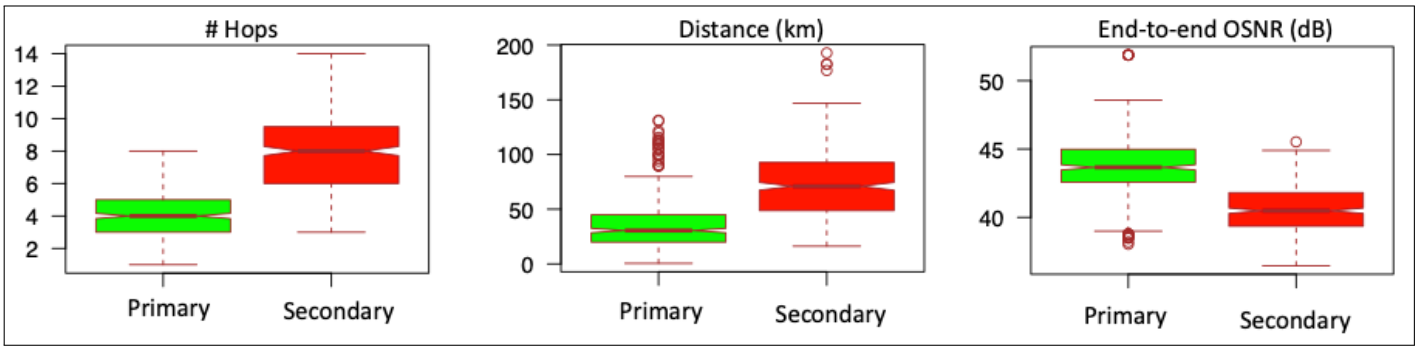

Fig. 9. Boxplots of number of hops, end-to-end distance and OSNR for primary (green) and secondary (yellow) paths.

Table 2. Percentage of lightpaths possible at 25 Gb/s, 40 Gb/s, and 50 Gb/s as topology grows in length

	Avg. link	Primary			Secondary		
α	length (Km)	25 Gb/s	40 Gb/s	50 Gb/s	25 Gb/s	40 Gb/s	50 Gb/s
1x	8.65	100%	100%	92.63%	100%	100%	80.0%
1.5x	12.98	100%	100%	86.58%	100%	98.68%	57.89%
2x	17.30	100%	94.73%	78.42%	100%	93.16%	45.79%
2.5x	21.63	100%	93.16%	67.89%	100%	88.68%	34.74%
3x	25.95	94.74%	87.11%	50.26%	94.74%	75.53%	19.47%
5x	43.25	81.84%	45.26%	24.47%	66.05%	9.74%	3.95%
8x	69.20	37.63%	20.53%	11.58%	6.84%	3.68%	1.32%

Finally, with the advent of Edge Computing, where it is expected that operators introduce small datacenters in many close-to-user HL4 nodes, the VCSEL-based architecture makes even more sense since it allows long-distance connections between HL4 nodes and HL1/2 where a subset of delay non-critical network functions are centralised at a few HL1/2 nodes.

7. SUPPLEMENTAL MATERIAL

The R code used in the experiments of Section 5 is publically available at GitHub:
https://github.com/josetilos/PASSION_WDM_planner

FUNDING

European Union H2020 project PASSION, grant no. 780326 (http://www.passion-project.eu/).

REFERENCES

1. "Metro network traffic growth: an architecture impact study," Tech. rep., Alcatel-Lucent Bell Labs, white paper (2013).
2. "Cisco Visual Networking Index (VNI) Complete Forecast Update, 2017–2022," Tech. rep., Cisco, white paper (2019).
3. J. A. Hernández, R. Sánchez, I. Martín, and D. Larrabeiti, "Meeting the traffic requirements of residential users in the next decade with current ftth standards: how much? how long?" IEEE Commun. Mag. **57**, 120–125 (2019).
4. "The Internet of Things: An Overview Understanding the Issues and Challenges of a More Connected World," Tech. rep., The Internet Society (ISOC) (2015).
5. F. Liu, G. Tang, Y. Li, Z. Cai, X. Zhang, and T. Zhou, "A Survey on Edge Computing Systems and Tools," Proc. IEEE **107**, 1537–1562 (2019).
6. J. A. Hernandez, M. Quagliotti, L. Serra, L. Luque, R. Lopez da Silva, A. Rafel, O. Gonzalez de Dios, V. Lopez, A. Eira, R. Casellas, A. Lord, J. Pedro, and D. Larrabeiti, "Comprehensive model for technoeconomic studies of next-generation central offices for metro networks," IEEE/OSA J. Opt. Commun. Netw. **12**, 414–427 (2020).
7. J. A. Hernandez, M. Quagliotti, E. Riccardi, V. Lopez, O. G. d. Dios, and R. Casellas, "A Techno-Economic Study of Optical Network Disaggregation Employing Open Source Software Business Models for Metropolitan Area Networks," IEEE Commun. Mag. **58**, 40–46 (2020).
8. E. Riccardi, P. Gunning, Óscar González de Dios, M. Quagliotti, V. López, and A. Lord, "An Operator view on the Introduction of White Boxes into Optical Networks," J. Light. Technol. **36**, 3062–3072 (2018).
9. J. Bäck, P. Wright, J. Ambrose, A. Chase, M. Jary, F. Masoud, N. Sugden, G. Wardrop, A. Napoli, J. Pedro, M. A. Iqbal, A. Lord, and D. Welch, "Capex savings enabled by point-to-multipoint coherent pluggable optics using digital subcarrier multiplexing in metro aggregation networks," in *2020 European Conference on Optical Communications (ECOC),* (2020), pp. 1–4.
10. J. Bäck, J. Pedro, T. Schaich, A. Napoli, P. Wright, A. Chase, D. Welch, and A. Lord, "Hubbedness: a metric to describe traffic flows in optical networks and an analysis of its impact on efficiency of point-to-multipoint coherent transceiver architectures," in *2021 European Conference on Optical Communication (ECOC),* (2021), pp. 1–4.
11. D. Welch, A. Napoli, J. Bäck, W. Sande, J. Pedro, F. Masoud, C. Fludger, T. Duthel, H. Sun, S. J. Hand, T.-K. Chiang, A. Chase, A. Mathur, T. A. Eriksson, M. Plantare, M. Olson, S. Voll, and K.-T. Wu, "Point-to-multipoint optical networks using coherent digital subcarriers," J. Light. Technol. **39**, 5232–5247 (2021).
12. M. Svaluto Moreolo, J. M. Fabrega, L. Nadal, R. Martinez, R. Casellas, J. Vilchez, R. Munoz, R. Vilalta, A. Gatto, P. Parolari, P. Boffi, C. Neumeyr, D. Larrabeiti, G. Otero, and J. P. Fernandez-Palacios, "Programmable VCSEL-based photonic system architecture for future agile Tb/s metro networks," IEEE/OSA J. Opt. Commun. Netw. **13**,

A187–A199 (2021).
13. M. S. Moreolo, L. Nadal, J. M. Fabrega, F. J. Vilchez, C. Neumeyr, A. Gatto, P. Parolari, and P. Boffi, "Multi-Tb/s photonic transceivers for metro optical network connectivity evolution," in *Metro and Data Center Optical Networks and Short-Reach Links IV,* vol. 11712 A. K. Srivastava, M. Glick, and Y. Akasaka, eds., International Society for Optics and Photonics (SPIE, 2021), pp. 36 – 42.
14. N. Sambo, P. Castoldi, A. D'Errico, E. Riccardi, A. Pagano, M. S. Moreolo, J. M. Fàbrega, D. Rafique, A. Napoli, S. Frigerio, E. H. Salas, G. Zervas, M. Nolle, J. K. Fischer, A. Lord, and J. P. F.-P. Giménez, "Next generation sliceable bandwidth variable transponders," IEEE Commun. Mag. **53**, 163–171 (2015).
15. R. Proietti, C. Qin, B. Guan, N. K. Fontaine, S. Feng, A. Castro, R. P. Scott, and S. J. B. Yoo, "Elastic optical networking by dynamic optical arbitrary waveform generation and measurement," J. Opt. Commun. Netw. **8**, A171–A179 (2016).
16. V. Katopodis, H. Mardoyan, C. Tsokos, D. Felipe, A. Konczykowska, P. Groumas, M. Spyropoulou, L. Gounaridis, P. Jennevé, F. Boitier, F. Jorge, T. K. Johansen, M. Tienforti, J.-Y. Dupuy, A. Vannucci, N. Keil, H. Avramopoulos, and C. Kouloumentas, "Multiflow transmitter with full format and rate flexibility for next generation networks," J. Light. Technol. **36**, 3785–3793 (2018).
17. M. Svaluto Moreolo, J. M. Fàbrega, L. Nadal, and F. J. Vílchez, "Exploring the potential of VCSEL technology for agile and high capacity optical metro networks," in *2018 International Conference on Optical Network Design and Modeling (ONDM),* (2018), pp. 254–259.
18. M. S. Moreolo, L. Nadal, J. M. Fabrega, F. J. Vilchez, C. Neumeyr, A. Gatto, P. Parolari, and P. Boffi, "VCSEL-based sliceable bandwidth/bitrate variable transceivers," in *Metro and Data Center Optical Networks and Short-Reach Links II,* vol. 10946 A. K. Srivastava, M. Glick, and Y. Akasaka, eds., International Society for Optics and Photonics (SPIE, 2019), pp. 26 – 32.
19. P. Parolari, A. Gatto, M. Rapisarda, C. Neumeyr, M. S. Moreolo, J. Fabrega, L. Nadal, and P. Boffi, "Effect of filtering in dense WDM metro networks adopting VCSEL-based multi-Tb/s transmitters," in *2019 21st International Conference on Transparent Optical Networks (ICTON),* (IEEE, 2019), pp. 1–4.
20. M. Svaluto Moreolo, J. M. Fabrega, L. Nadal, R. Martínez, and R. Casellas, "Synergy of photonic technologies and software-defined networking in the hyperconnectivity era," J. Light. Technol. **37**, 3902–3910 (2019).
21. A. Eira, J. Pedro, and J. J. Pires, "Modeling cost versus flexibility in optical transport networks," J. Light. Technol. **37**, 61–74 (2019).
22. M. S. Moreolo, R. Martinez, J. M. Fabrega, R. Casellas, J. Vilchez, L. Nadal, R. Vilalta, R. Munoz, C. Neumeyr, H. D. Jung, J. U. Shin, A. Gatto, P. Parolari, P. Boffi, D. Larrabeiti, and J. P. Fernandez-Palacios, "Demonstration of an SDN-enabled VCSEL-based photonic system for spectral/spatial connectivity in disaggregated optical metro networks," in *2021 Optical Fiber Communications Conference and Exhibition (OFC),* (2021).
23. D. J. Ives, A. Alvarado, and S. J. Savory, "Throughput gains from adaptive transceivers in nonlinear elastic optical networks," J. Light. Technol. **35**, 1280–1289 (2017).
24. D. Larrabeiti, J. Fernández-Palacios, G. Otero, M. S. Moreolo, J. M. Fabrega, R. Martínez, P. Reviriego, and V. López, "All-optical paths across multiple hierarchical levels in large metropolitan area networks," in *2019 Asia Communications and Photonics Conference (ACP),* (IEEE, 2019), pp. 1–3.
25. "METRO high bandwidth, 5G application-aware optical network, with edge storage, compute and low latency (METRO-HAUL) project website," https://metro-haul.eu/. Accessed: 2020-10-03.
26. D. Larrabeiti, G. Otero, J. A. Hernández, P. Reviriego, J. Fernández-Palacios, V. López, M. Svaluto Moreolo, R. Martínez, and J. M. Fábrega, "Tradeoffs in optical packet and circuit transport of fronthaul traffic: the time for SBVTs?" in *in Proceedings of 24th conference on Optical Network design and Modelling (ONDM2020), May 18-21 , Castelldefels/virtual, Spain,* (2019).
27. G. Otero, D. Larrabeiti, J. A. Hernández, P. Reviriego, J. P. Fernández-Palacios, V. López, M. Svaluto-Moreolo, J. M. Fabrega, L. Nadal, and R. Martínez, "Optical interconnection of CDN caches with Tb/s sliceable bandwidth-variable transceivers featuring dynamic restoration," in *2019 European Conference on Networks and Communications (EuCNC),* (2019), pp. 69–72.
28. G. Otero, J. P. Fernández-Palacios, M. S. Moreolo, D. Larrabeiti, J. A. Hernandez, J. M. Fabrega, V. Lopez, L. Nadal, and R. Martinez, "Scaling edge computing through S-BVT and Pb/s switching devices in large dense urban metro networks," in *2020 22nd International Conference on Transparent Optical Networks (ICTON),* (2020), pp. 1–5.
29. A. Gatto, P. Parolari, P. Martelli, and P. Boffi, "Vcsel-based communications for metro and access networks," in *2018 Photonics in Switching and Computing (PSC),* (2018), pp. 1–3.
30. G. Delrosso and S. Bhat, "Development and scalability of a 2 tb/s data transmission module based on a <tex>$3\ \mu\mathrm{m}$</tex> soi silicon photonics platform," in *2020 22nd International Conference on Transparent Optical Networks (ICTON),* (2020), pp. 1–5.
31. R. Martinez, R. Casellas, M. Svaluto Moreolo, J. M. Fabrega, R. Vilalta, R. Munoz, L. Nadal, V. Lopez, J. P. Fernandez-Palacios, D. Larrabeiti, and G. Otero, "Experimental evaluation of an on-line rsa algorithm for sdn-controlled optical metro networks with vcsel-based s-bvts," in *2020 International Conference on Optical Network Design and Modeling (ONDM),* (2020), pp. 1–6.
32. P. Parolari, A. Gatto, M. Rapisarda, F. Lipparini, C. Neumeyr, M. S. Moreolo, and P. Boffi, "Preliminary assessment of photonic solutions based on C-band VCSELs for multi-Tb/s metro networks," in *2020 22nd International Conference on Transparent Optical Networks (ICTON),* (IEEE, 2020), pp. 1–5.
33. M. Rapisarda, A. Gatto, P. Martelli, P. Parolari, C. Neumeyr, M. Svaluto Moreolo, J. M. Fabrega, L. Nadal, and P. Boffi, "Impact of chirp in high-capacity optical metro networks employing directly-modulated VCSELs," in *Photonics,* vol. 5 (Multidisciplinary Digital Publishing Institute, 2018), p. 51.
34. R.-J. Essiambre, G. Kramer, P. J. Winzer, G. J. Foschini, and B. Goebel, "Capacity limits of optical fiber networks," J. Light. Technol. **28**, 662–701 (2010).
35. R. Stabile, N. Tessema, K. Prifti, D. W. Feyisa, B. Shi, and N. Calabretta, "Photonic integrated nodes for next-generation metro optical networks," in *Metro and Data Center Optical Networks and Short-Reach Links IV,* vol. 11712 A. K. Srivastava, M. Glick, and Y. Akasaka, eds., International Society for Optics and Photonics (SPIE, 2021), pp. 55 – 60.
36. P. S. Chow, J. M. Cioffi, and J. A. Bingham, "A practical discrete multitone transceiver loading algorithm for data transmission over spectrally shaped channels," IEEE Transactions on communications **43**, 773–775 (1995).
37. A. Alvarado, D. J. Ives, S. J. Savory, and P. Bayvel, "On the impact of optimal modulation and FEC overhead on future optical networks," J. Light. Technol. **34**, 2339–2352 (2016).